







Tuning Proton Exchange Membrane Electrolytic Cell Performance by Conditioning Nafion N115-Based Membrane Electrode Assemblies

Niklas Wolf^{1,2} \bigcirc | Ali Javed¹ | Leander Treutlein^{1,2} \bigcirc | Hans Kungl¹ | André Karl¹ | Eva Jodat¹ | Rüdiger-A Eichel^{1,2,3}

¹Institute of Energy Technologies, Fundamental Electrochemistry (IET-1), Forschungszentrum Jülich, Juelich, Germany | ²Institute of Physical Chemistry, RWTH Aachen University, Aachen, Germany | ³Faculty of Mechanical Engineering, RWTH Aachen University, Aachen, Germany

Correspondence: Niklas Wolf (n.wolf@fz-juelich.de)

Received: 7 October 2024 | Revised: 17 December 2024 | Accepted: 20 December 2024

Funding: This study was supported by German Federal Ministry of Education and Research (BMBF) within the H_2 Giga project DERIEL (grant number 03HY122C).

Keywords: break-in | MEA conditioning | pre-treatment | proton exchange membrane electrolyser

ABSTRACT

Conditioning of the membrane electrode assembly (MEA) is an important step to establish functionality and obtain a consistent performance of the proton exchange membrane electrolytic cell (PEMEC) when setting it into operation. On a laboratory scale in an academic context, conditioning encompasses primary pre-treatment of the MEA by chemical or thermal procedures under defined mechanical conditions and, secondarily, the break-in procedure, during which the PEMEC is subjected to initial electrical loads before actual operation. This study demonstrates the effect of MEA conditioning on the short-term performance of PEMEC. The impact of mechanical, chemical and thermal conditions during pre-treatment was investigated for Nafion N115-based MEAs while keeping the break-in procedure invariant for all pre-treatment conditions. The electrochemical characterisation was performed using polarisation curves and electrochemical impedance spectroscopy. The impact of ex situ-before assembly of the cell-versus in situ-after assembly of the cell-conditioning resulted in markedly different mechanical conditions. The experimental results showed an improvement in PEMEC performance by pre-treating the MEA after cell assembly. Compared to pre-treatment with deionised water (DI water) at 60°C, treatment with acidic solution improved the performance, evidenced by a 21 mV reduction in cell voltage at 2 A·cm⁻². When compared with DI water at 60°C, a pre-treatment at 90°C with DI water reduced cell voltage by 23 mV.

1 | Introduction

To ramp up a green hydrogen economy [1–3], proton exchange membrane (PEM) water electrolysis is generally considered as key enabling technology for chemical energy storage via power-to-gas and power-to-liquid processes [4]. PEM water electrolysis has several attractive features, such as its high energy efficiency

of up to 80%-90% under low temperature operation 20°C - 80°C , compact balance of plant, efficient scalability, highly dynamic and fast response assuring compatibility with intermittently available renewably generated power [5, 6]. Although this technology is already commercially available, challenges remain related to low-cost manufacturing and degradation of the cell components. In order to characterise alternative cell component materials and

 $[Correction\ added\ on\ 2\ April\ 2025,\ after\ first\ online\ publication:\ an\ additional\ affiliation\ for\ the\ seventh\ author\ has\ been\ added\ in\ this\ version.]$

This is an open access article under the terms of the Creative Commons Attribution License, which permits use, distribution and reproduction in any medium, provided the original work is properly cited.

© 2025 The Author(s). Electrochemical Science Advances published by Wiley-VCH GmbH.

predict the lifetime under reliable operating conditions, a universal method to define the steady state at the beginning of operation (BOO) of a running electrolyser is urgently needed. During the BOO phase, the performance of the electrolyser is volatile because the system needs time to fully stabilise. Therefore, stable voltage should be considered when comparing different alternatives of cell materials and calculating the degradation rate instead of the voltage at the BOO.

In the BOO phase, the performance of PEM electrolytic cell (PEMEC) might be inconsistent, which can be optimised by properly conditioning the membrane electrode assembly (MEA). The MEA is an indispensable component of PEMEC, which is comprised of a primary inner layer, the PEM. This membrane is coated with a typically iridium-based catalyst on the anode side, whereas platinum-based catalysts are typically used on the cathode side. Conditioning of the MEA is a very diverse process, which is already actively utilised in PEM fuel cells [7-11]. This field is also the subject of recently published studies, and some insights have already been gained. For PEMFC applications, the removal of solvents from production and the changes in the catalyst layer ionomer appear to be relevant factors in the activation process [12]. Furthermore, several publications show that the constant voltage method is a faster and more gentle conditioning method for fuel cells than the constant current method. This is explained by less agglomeration of the platinum nanoparticles in the cathode catalyst layer and less reduction of the electrochemical surface area of the activated MEA [7, 13]. In the field of PEM electrolysers, EIS and Tafel slope have been used to show that both ohmic and activation overvoltage losses decrease after conditioning [14]. However, its implementation in PEMEC is quite minimal so far. The European Union (EU) has recommended a list of harmonised protocols regarding cell design, characterisation and evaluation of electrolysis systems to further develop the PEMEC technology [15–18]. Nevertheless, no standard method in the context of MEA conditioning has been highlighted [18]. For both the galvanostatic operation at 1 A·cm⁻² [19] and the potentiostatic operation at 1.8 V [20], a decrease in cell performance can be observed during the first hours of operation. In contrast, other researchers observed an improvement in performance in galvanostatic operation at the start of the experiment [21]. Of course, all operating parameters and MEA properties, such as membrane type and catalyst loading, must also be considered when evaluating these changes. It can be concluded that the use of conditioning procedures is not yet consistently used in PEM electrolysis research and can be a reason for deviations between experimental results.

Another study has emphasised the high-priority need for conditioning and standardisation by conducting a round-robin test effort at five different laboratories. Although the same characterisation and hardware framework were employed, differences in the results were noted [22]. The benefits of utilising conditioning in PEMEC, particularly in reducing ohmic resistance and activation overpotential losses, have been demonstrated in previous studies [14]. Further investigations into the changes in the mechanical properties of the MEA during pre-treatment were also conducted [23].

In this study, we address the conditioning as an initial processing step to 'activate' the MEA [24] and prepare it for optimal perfor-

mance. For activation, the MEA was hydrated via a 'pre-treatment procedure' and electrochemically activated via a 'break-in procedure'. Pre-treatment may include the exposure of the MEA to hot or cold water and thereby exerting thermal impacts on the MEA. Alternatively, the exposure with H₂O₂ and acidic solution of H₂SO₄ may induce chemical impacts [11, 25]. On the other hand, during the break-in procedure, either galvanostatic or potentiostatic mode is applied for a defined time to stabilise the PEMEC operation [22, 26, 27]. In this work, we discuss how differences in the conditioning procedure influence the shortterm electrochemical performance of a PEMEC. We propose that the mechanical, chemical and thermal conditions applied during the pre-treatment significantly affect the contact resistance and membrane conductivity. In situ conditioning, which allows for membrane swelling under confined conditions, leads to an improved contact area with the PTLs. The combination of thermal and chemical pre-treatment can enhance the membrane's proton conductivity, contributing to a decrease in ohmic resistance and overall cell voltage during constant current operation.

2 | Experimental

The water electrolysis experiments were performed on an inhouse built single cell, shown in Figure 1. Four electrolysis cells were operated simultaneously with four commercial HYDRion MEAs, purchased from Ion Power GmbH. The MEA comprises a Nafion N115 membrane with a catalyst loading of 1.0 mg/cm² IrOx on the anode side and 0.3 mg/cm² Pt on the cathode side. Nafion was used as a binder in the catalyst layers. The active area of the MEA is 4.4×4.4 cm². For the anode side, one layer (250 μ m thick) of the CURRENTO 2GDL10N-0.25 porous transport layer (PTL) was utilised. Both sides of PTL were platinum-coated, with the coating thickness specified as 0.2 µm, provided by the manufacturer NV Bekaert SA. For the cathode, one layer of PTL of Toray carbon paper TGP-H-60 sourced from Alfa Aesar was utilised. The remaining cell components were based on an inhouse cell design. The bipolar plates, featuring a parallel flow field design, were made of titanium grade 2. The anode side of these plates was coated with platinum with a nominal thickness of 2.5 µm, whereas the cathode side was coated with gold with a nominal thickness of 2.5 µm. These coatings were applied by METAKEM GmbH. To avoid leakage of the cell, PTFE gaskets were used. The thickness of the gaskets was matched to the thickness of the PTLs, with a thickness of 200 µm for the anode and 300 μm for the cathode. Stainless steel was used to fabricate the end plates. The applied torque for clamping the cell was 5 Nm.

2.1 | Test Station

Four test stations were developed in-house and installed to conduct four experiments concurrently. Figure 2 shows the schematic diagram of one test station. Each side of the cell was individually heated by a pair of heating rods, which are regulated by a single temperature sensor per side. The gas—liquid separators, serving as water reservoirs, were heated and controlled by PTFE-coated temperature sensors. All heating devices were purchased from Pohltechnic.com GbR. The peristaltic pumps in the system include a pump drive and stainless-steel pump heads from Masterflex. The internal tubing of the pumps is composed of



FIGURE 1 | Components of a dismantled laboratory-based single cell proton exchange membrane electrolytic cell, including: (1) end plate, (2) flow field (anode), (3) flow field (cathode), (4) porous transport layer (anode), (5) porous transport layer (cathode), (6) sealings, (7) water inlet/outlet, (8) electrical isolation and (9) connection for power cable. The commercially bought membrane electrode assembly was compressed between the anode and the cathode components of cell.

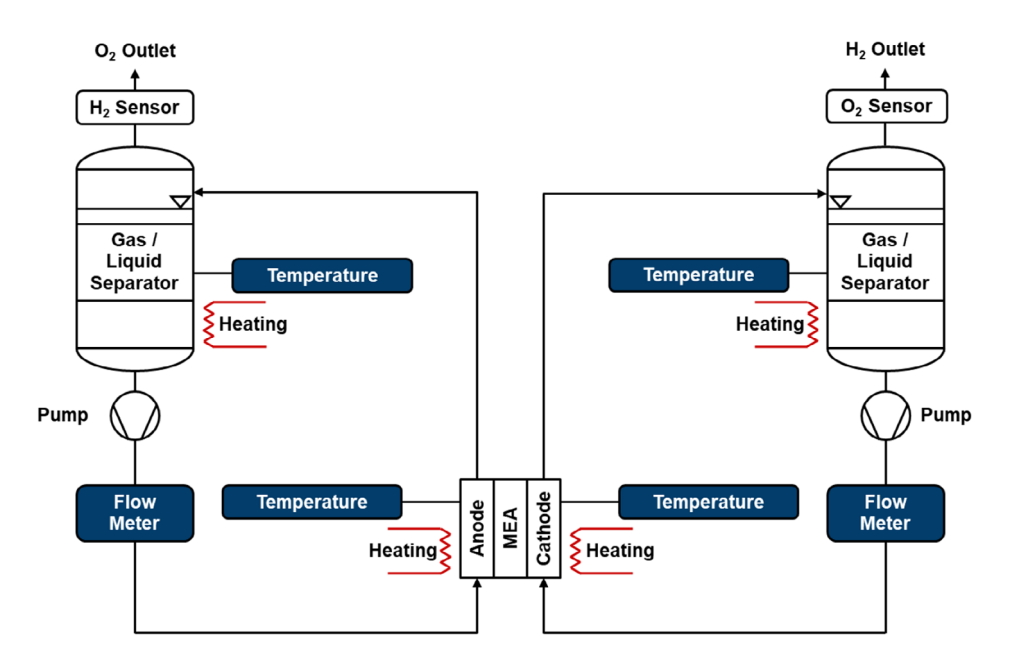


FIGURE 2 | Schematic diagram of in-house developed test station to operate single PEMEC.

Norprene, whereas the external tubing is made up of PTFE. The design of the equipment allows to set operating parameters such as flow rate and temperature in a workflow and control them automatically during the experiment. The electrochemical measurements and power supply were facilitated by VMP-300 potentiostats from Biologic, each equipped with 6×10 A boosters and a single electrochemical impedance spectroscopy channel per cell.

2.2 | Conditioning Procedures

Four different pre-treatment procedures were investigated by using the same break-in procedure, summarised in Figure 3. In

the first procedure, the MEA was first assembled in the cell and then hydrated in situ with deionised water for 12 h at 60° C. In the second procedure, the MEA was initially soaked in deionised water for 12 h at 60° C ex situ, followed by assembling it in the cell under a wet state. The comparison between these two procedures should provide insight into mechanical effects on the MEA during conditioning. In the next procedure, the MEA was assembled in the cell and pre-treated in situ similar to references [11, 22, 26], by supplying hydrogen peroxide (H_2O_2) for 1 h, deionised water for 1 h, 0.5 mol•L⁻¹ sulphuric acid (H_2SO_4) for 1 h, and subsequently deionised water for 12 h at 60° C. The comparison between the pre-treatment procedures with water and acids can help to understand the chemical impacts on the

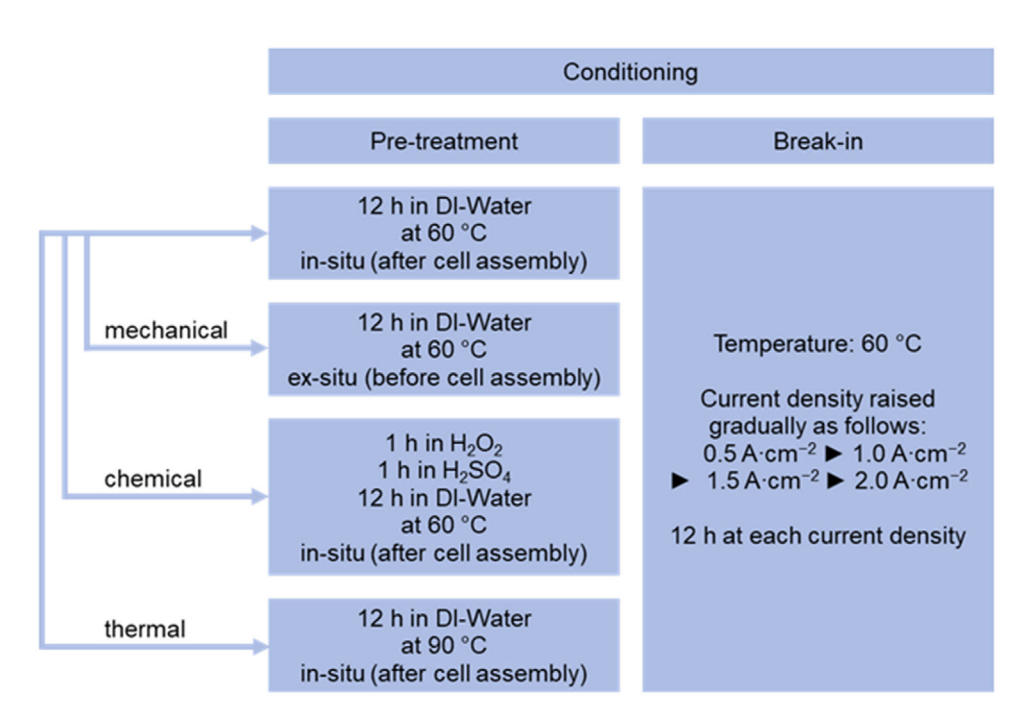


FIGURE 3 Overview of explored conditioning procedures. Each procedure was applied on pristine membrane electrode assembly. [Correction added on April 2, 2025, after first Online publication: figure 3 has been updated in this version.]

MEA during conditioning. In the last procedure, after assembling in the cell, the MEA was subjected in situ to hydration with deionised water for 12 h at 90°C. The comparison between the pretreatment procedures at 60°C and 90°C is intended to investigate the thermal impacts on the MEA during conditioning. After pre-treating the MEA, the break-in procedure was applied by installing the PEMEC in the respective test stand and circulating high-purity water with a flow rate of 0.05 L⋅min⁻¹ continuously on both sides of the cell; the anode and the cathode. Four different current densities, 0.5, 1.0, 1.5 and 2.0 A⋅cm⁻², were applied to the cell for 12 h each in an ascending order. Each cell was operated at 60°C. For each of the four current density steps, electrochemical impedance spectroscopy measurements were carried out at the current density of the corresponding step and each lower current density. Afterwards, a polarisation curve from 0.0001 A·cm⁻² up to the current density of the corresponding step was measured. The current density was then kept constant at the corresponding step for 3 h. This process was repeated three times. Then, the next current density was applied, and the above-mentioned steps were repeated until the operation at all four current densities was completed. An illustration of break-in procedure is presented in Figure S1.

2.3 | Electrochemical Characterisation

Each cell was electrochemically characterised via recording a polarisation curve (IV-curve) and electrochemical impedance spectroscopy (EIS). Polarisation curves were measured in galvanostatic mode by increasing current densities in a stepwise manner and holding each step for a duration of one minute. The potential was recorded every second, but only the last ten data points for each applied current density step were utilised for analysis. To achieve a high resolution at low current densities, the step size was increased logarithmically. The lowest current

density applied was $0.0001~\text{A}\cdot\text{cm}^{-2}$, which was incrementally increased up to $0.001~\text{A}\cdot\text{cm}^{-2}$ with a step size of $0.0001~\text{A}\cdot\text{cm}^{-2}$. Between $0.001~\text{and}~0.01~\text{A}\cdot\text{cm}^{-2}$, the step size was $0.001~\text{A}\cdot\text{cm}^{-2}$; between $0.01~\text{and}~0.1~\text{A}\cdot\text{cm}^{-2}$, it was $0.01~\text{A}\cdot\text{cm}^{-2}$; and between $0.1~\text{and}~2~\text{A}\cdot\text{cm}^{-2}$, it was $0.01~\text{A}\cdot\text{cm}^{-2}$. The shunt was switched at $0.01~\text{A}\cdot\text{cm}^{-2}$ to enhance resolution at very low current densities. Moreover, EIS was performed in galvanostatic mode at regular intervals during the experiments. The applied direct current (DC) density varied depending on the corresponding break-in stage, being either $0.5, 1.0, 1.5~\text{or}~2.0~\text{A}\cdot\text{cm}^{-2}$. According to the literature the alternating current (AC) amplitude is set to 10% of the DC current [28], and the frequency ranged from 500~kHz to 0.1~Hz.

3 | Results and Discussion

3.1 | Mechanical Impact

This section presents the electrochemical characterisation of two MEAs that were pre-treated either before (in the following: ex situ) or after (in the following: in situ) cell assembly using deionised water. Figure 4a shows the voltages recorded during the galvanostatic break-in procedure as a function of time. It is evident that, even at 0.5 A·cm⁻², lower voltages were measured for the MEA pre-treated in situ. The voltage gap between the two MEAs further increases as the current density increases. This change in voltage is also observed in the polarisation curves, shown in Figure 4b. Clearly, the voltage gap expands by increasing the current density [29], resulting in a difference of approximately 30 mV at a current density of 2 A·cm⁻². This might be related to the time needed to reach steady state. A time-dependent effect would suggest continuous formation of additional proton-conductive water channels, thereby enhancing proton conductivity and reducing ohmic resistance [30]. However, multiple polarisation curves (Figure S2) during each current

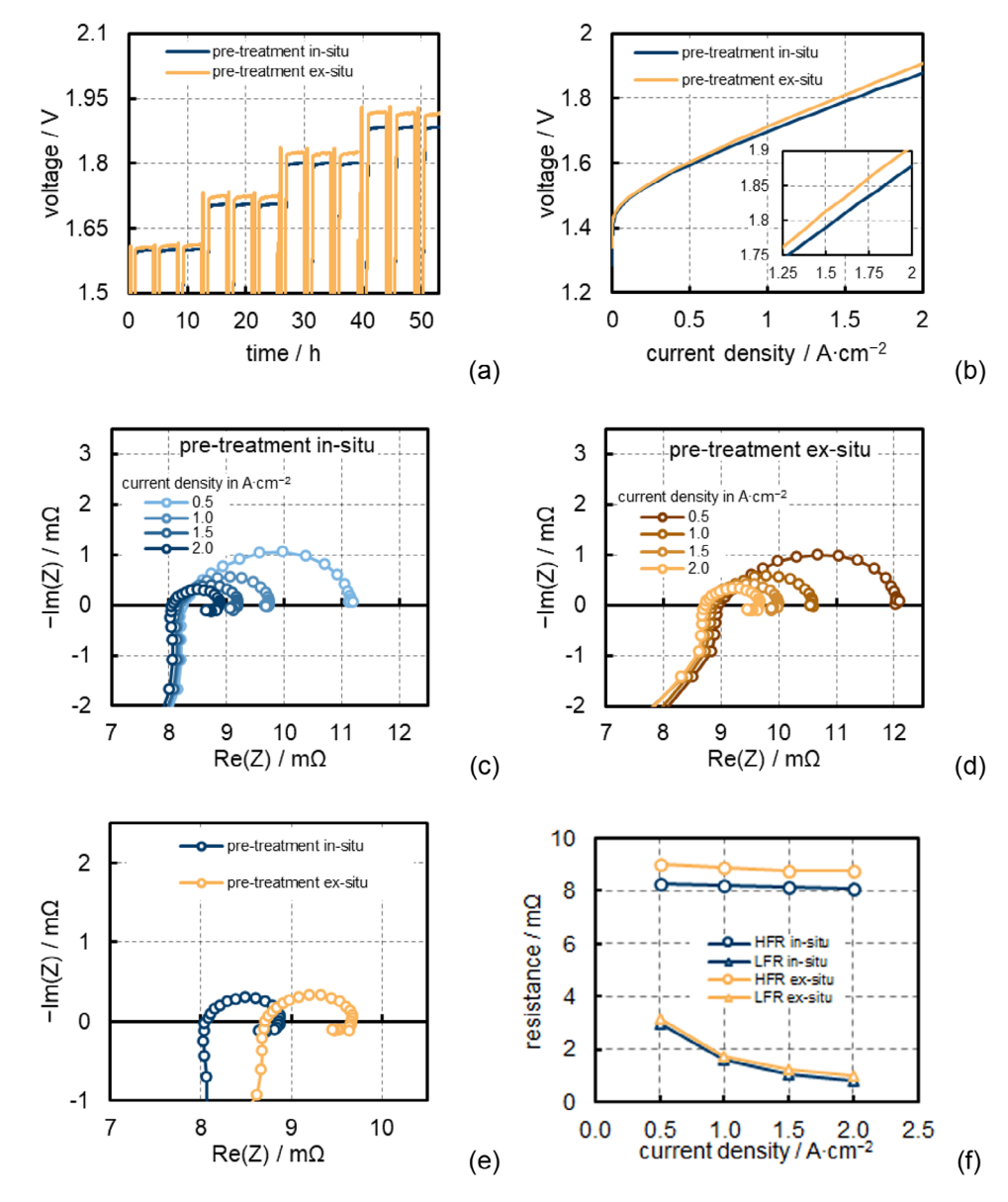


FIGURE 4 | Comparison of the break-in procedure between the MEAs pre-treated after (blue) and before (orange) cell assembly. (a) Cell voltage recorded throughout time, (b) polarisation curves measured at the end of break-in, (c) impedance measured at different current densities for the MEA hydrated after cell assembly, (d) impedance measured at different current densities for MEA hydrated before cell assembly, (e) comparison of impedance for both MEAs at 2 A·cm⁻² and (f) ohmic resistance and charge transfer resistance calculated after fitting the impedance spectra via an equivalent circuit model. [Correction added on April 2, 2025, after first Online publication: figure 4(f) has been updated in this version.]

density step indicate no significant changes, suggesting that the ohmic resistance for each MEA remains constant within the measurement accuracy. Therefore, the voltage gap between two MEAs can be attributed to a change in ohmic resistance caused by the pre-treatment procedure.

To validate that the difference in pre-treatment procedures influences the ohmic resistance, EIS was performed before measuring polarisation curves. Figure 4c,d shows the Nyquist plots (imaginary vs. real part of impedance) for both MEAs, respectively. The capacitive part of each plot consists of only one depressed semicircle at each applied DC current density that allows us to determine the ohmic resistance (R_{Ω}) from the high-frequency intercept and the charge transfer resistance from the low-frequency intercept ($R_{\rm CT}$). Both parameters were calculated

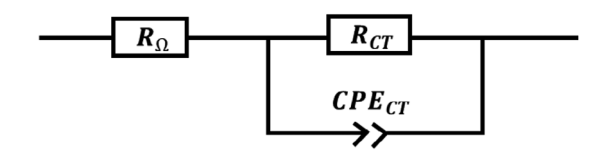


FIGURE 5 | Equivalent circuit model used to fit the depressed semicircle for all pre-treatment procedures. Here, R_{Ω} represents the ohmic resistance, R_{CT} stands for the charge transfer resistance and CPE_{CT} denotes the constant phase element.

by fitting an appropriate equivalent circuit model, shown in Figure 5. Both plots represent that by increasing the applied DC current density, the $R_{\rm CT}$ decreases substantially, which can be calculated by the Butler-Volmer equation [31]. In contrast, the $R_{\rm O}$

decreases slightly. Figure 4e shows a comparison of impedance spectra at $2 \text{ A} \cdot \text{cm}^{-2}$. By fitting the spectra, the R_{Ω} for the MEAs pretreated in situ and ex situ were calculated as, 8.07 and 8.73 m Ω , respectively. Figure 4f depicts a comprehensive view of the R_{Ω} and the R_{CT} for both MEAs at different current densities. The change in R_{CT} is rather minor, while in the R_{Ω} is approximately 8.1%. This discrepancy in the R_{Ω} may be attributed to the contact resistance between the cell components. The ionic conductivity of the membrane essentially relies on its hydration state [32], which differs with the change in the number of water molecules per sulphonate group.

For instance, 3 water molecules represent the lower hydration state, 20 water molecules reflect the intermediate hydration state and beyond 20 water molecules define the higher hydration state [33]. The membrane's swelling behaviour transforms upon the hydration state characteristic, hence tailoring the mechanical properties of the membrane [34-36]. Since both MEAs were subjected to the same temperature during the pre-treatment, we presume that there is no difference in their hydration states [37, 38]. However, the MEA pre-treated in situ was hydrated under a constrained environment (after cell assembly; confined within cell geometry), and the MEA pre-treated ex situ was hydrated under an unrestricted environment (before cell assembly; no external constraint). Due to these distinctions, it is possible that both MEAs have different swelling ratios, not only along the in-plane dimension but also along the through-plane dimension. This may influence the contact resistance between MEA and PTLs.

Figure 6 exemplifies how the contact between MEA and PTL could develop when assembling the PEMEC. The PTLs are featured with an inhomogeneous surface comprising tiny crowns and cavities. Hence, the MEA pre-treated ex situ may merely establish the contact with the crowns, leading to higher contact resistance. On the contrary, the expansion of the membrane under a confined environment might have emerged as an improved contact between the MEA and the PTLs on both sides, anode and cathode, illustrated in Figure 6a. Within this context, the catalyst particles drive into the porous surface of the PTL by the mechanical force and possibly increase the contact area. Another factor that can improve the contact between MEA and PTL is an increase in clamping pressure. Insights from a study of 2019 highlight the critical role of PTL microstructure, including porosity, in contact resistance and electrochemical performance. In line with these findings, the different contact behaviour between the MEAs can be attributed to the varying deformation and expansion of the membrane during conditioning. The improved contact area for the in situ conditioned MEA could thus be facilitated by a porous PTL structure, allowing the ionomer-containing catalyst layer to expand in the cavities, contributing to enhanced electrochemical performance [39, 40]. However, experimental findings suggest that the compression pressure applied during PEMEC assembly does not have a substantial impact on the contact resistance [23]. A recent simulation study demonstrated in an illustrative way the stress and strain that a MEA encounters during cell assembly. The deformation of the MEA responsible for the decrease in R_{Ω} was mainly related to the water uptake and swelling of the MEA rather than the clamping pressure during cell assembly [41]. Another investigation reveals that while the MEA expands, the PTLs also undergo compression [23]. The electrical resistance of the PTL decreases due to the compression and the reduced porosity [42].

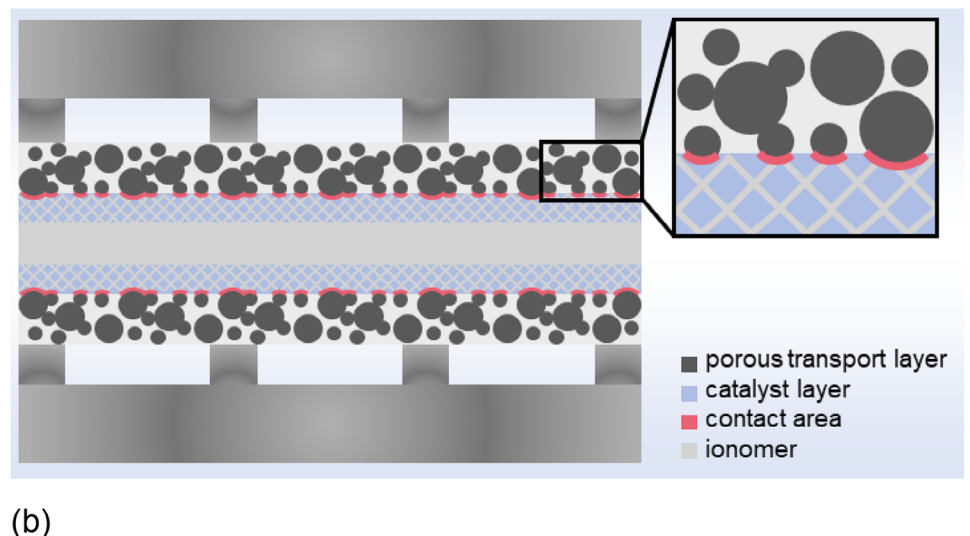
This implies that the contact resistance between the MEA pretreated in situ and the PTLs decreases due to the swelling of the MEA and compression of the PTLs. Only a fraction of these advantages can be utilised in the MEA pre-treated ex situ, which was initially able to expand without restriction and has only a little expansion potential after subsequent cell assembly.

3.2 | Chemical Impact

The pre-treatment of the MEA with sulphuric acid has already been explored, initially in PEM fuel cells [11] and later also in PEM electrolysers [31], because it improves the ion conductivity by increasing the number of protons of the Nafion membrane. Applying this procedure in a modified way, a pristine MEA was pre-treated with H₂O₂ and H₂SO₄ (in the following: acidic). Figure 7 represents the comparison of electrochemical results between the MEA pre-treated with water in situ at 60°C (deionised water) and the MEA pre-treated with acids in situ at 60°C (acidic). The voltage versus time plot shows that the MEA pre-treated with acids generated lower cell voltages compared to the MEA pre-treated with deionised water, as shown in Figure 7a. This means acidic pre-treatment has improved the PEMEC performance, which can also be seen in terms of the polarisation curve in Figure 7b. Here again, the gap between the two voltages slightly broadens with increasing current density. Figure 7f depicts the change in R_{Ω} (calculated via the equivalent circuit model) by changing the current density for both MEAs. This direct comparison indicates that R_{Ω} of the MEA pretreated with acids starts to mildly decrease beyond 1 A·cm⁻², which provides the rationale for the voltage gap stated above. Considering the accuracy of the EIS measurement, the R_{Ω} seems to decrease by approximately 7.04% at 2 A·cm⁻². On the other hand, the difference in charge transfer resistance between both MEAs exhibits only insignificant change, as shown in Figure 7e and Figure 7f. This decrease in R_{Ω} leads to a drop in cell voltage of approximately 21 mV at 2 A·cm⁻².

Generally, two conceivable mechanisms have to be distinguished; either an acidic pre-treatment decreases the R_{Ω} due to an increase in ionic conductivity of the membrane or a decrease in contact resistance between the MEA and PTLs. In literature, two possible reasons for the positive effect of the acidic pre-treatment on the Nafion membrane are outlined. Firstly, a pre-treatment with H₂O₂ removes organic contaminants on the catalyst surface left from industrial MEA fabrication [43], thereby improving contact resistance. Secondly, pre-treatment with H₂SO₄ enhances cell performance by replacing the metal cations like Na⁺ [44] bound in the membrane with the protons from the sulphuric acid. Hence, the proton conductivity increases as the number of mobile protons in the membrane increases [11]. Furthermore, the reorganisation of the hydrophilic domains improves the ionic conductivity of the membrane [45–47]. The pre-treatment of the membrane either with DI water or with H2SO4 influences the membrane thickness in a similar manner [31]. Therefore, we anticipate similar change in the thickness for both membranes since the two MEAs were subjected to pre-treatment after the cell assembly. Under this view, the decrease in R_{Ω} mainly is ascribed to the conductivity.

(a)



(5)

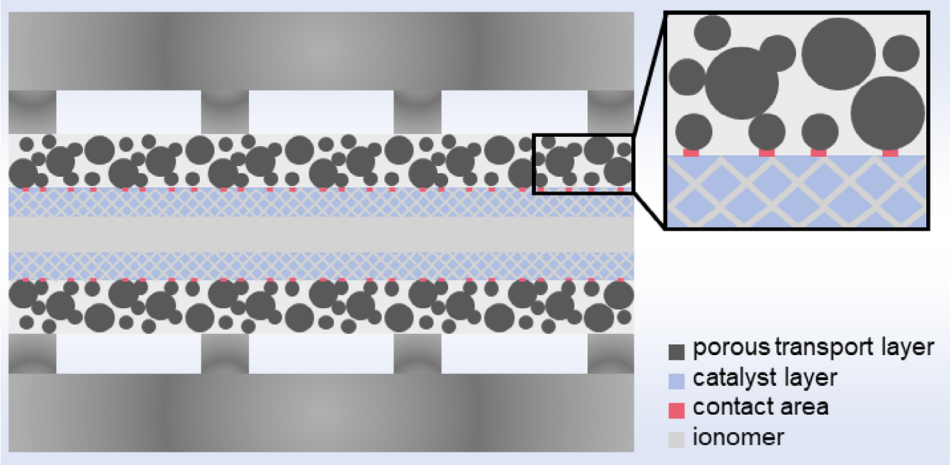


FIGURE 6 Schematic drawing of contact details between the MEA and the PTL. The ionomer, which is used as a binder in the catalyst layers, is shown in schematic way. (a) MEA pre-treated after cell assembly, (b) MEA pre-treated before the cell assembly. Here, the primary focus is on the contact surface area (red). For the MEA pre-treated in situ, the catalyst surface penetrates the porous surface of PTL due to MEA swelling upon hydration after the cell assembly, which improves the contact area.

3.3 | Thermal Impact

Figure 8 presents a comparative view of two MEAs pre-treated in situ at 60°C and 90°C concerning their electrochemical results. Figure 8a shows the voltage versus time plot with a distinct decrease in cell voltage at all applied current densities for the 90°C treated MEA. A comparable difference can also be noticed in the polarisation curves, displayed in Figure 8b. Contrary to the comparison described in Section 3.1 (Figure 4a) and Section 3.2 (Figure 7a), the voltage gap between the MEAs pre-treated at 60°C and 90°C remains approximately constant over time (Figure 8a). Figure 8c indicates a slight shift in R_{Ω} , whereas Figure 8d shows no change in R_{Ω} . However, accounting for the accuracy, the R_{Ω} is reduced by approximately 7.43% at 2 A·cm⁻² by pre-treating the MEA at 90°C (Figure 8f). This reduction leads to a decrease in cell voltage of about 23 mV at 2 A·cm⁻².

Comparing the experimental results of the MEA pre-treated in situ at 60°C and 90°C, there are three questions that will be

considered in detail now: why did the R_{Ω} reduce when comparing the performance of the MEA pre-treated at 60°C and 90°C (Question 1), why did the pre-treatment of MEA at 90°C not show any change in the R_{Ω} with increasing current density (Question 2) and did the exerted temperature influence the contact resistance due to thermal expansion (Question 3). It is well known that water uptake of a NAFION membrane is dependent on temperature, either subjected to humidity or immersed in the bulk water [38]. Contrary to the saturated water vapour, the water uptake in the liquid water is higher [32, 48]. To equilibrate the membrane in bulk water, water uptake varies with the pre-treatment procedure [32, 48, 49]. The pre-treatment of a NAFION membrane with deionised water at high temperature allows it to absorb more water by increasing the accessibility of sulphonic acid sites to water molecules, which enhances the number of water molecules per sulphonic acid site. Consequently, the ionic conductivity of the membrane enhances [48]. This could be a reason that the MEA pre-treated at 90°C performed better than the MEA pretreated at 60°C. During electrolysis operation, the membrane also

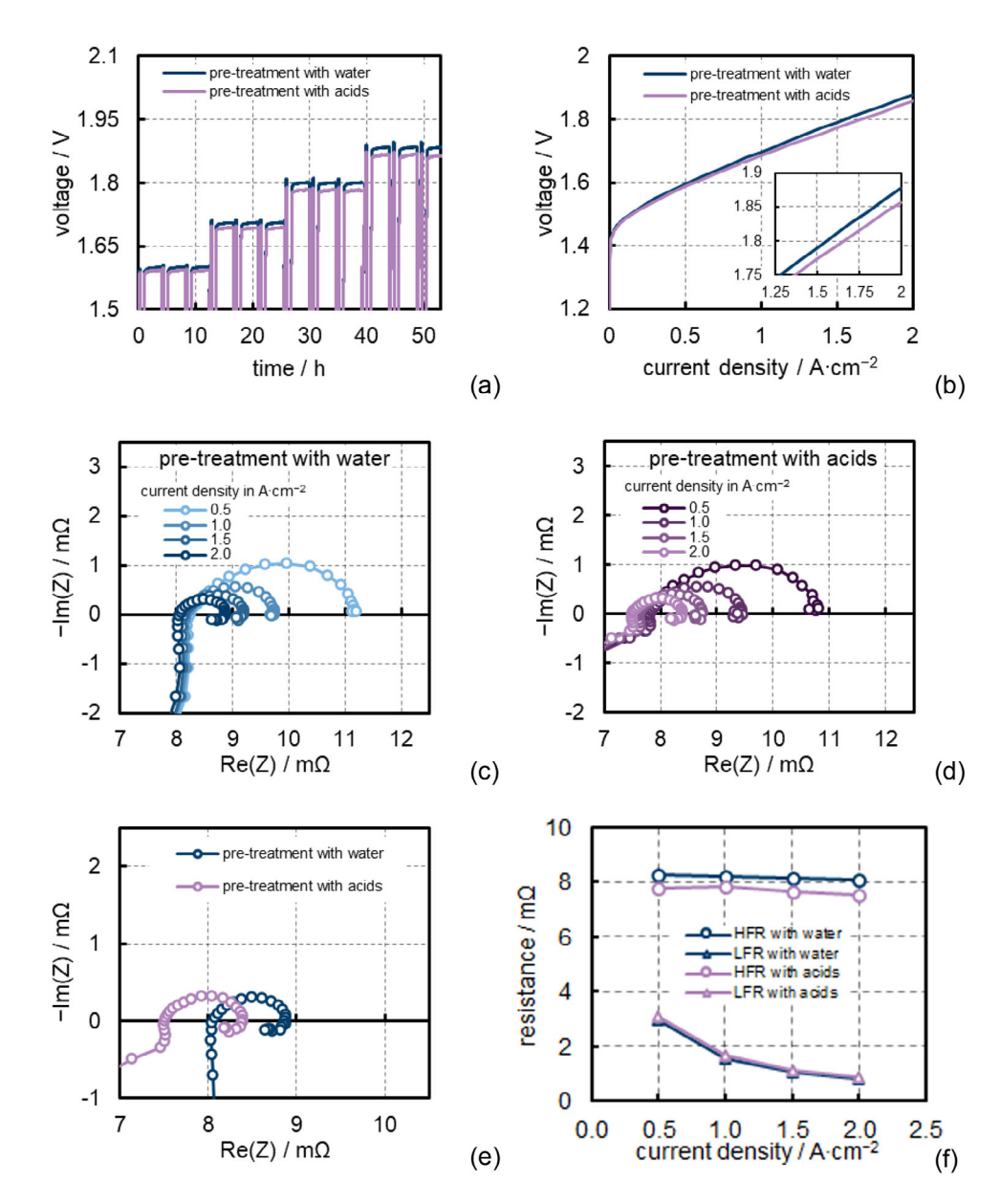


FIGURE 7 | Comparison of the break-in procedure between the MEAs pre-treated with deionised water (blue) and acidic solution (purple) after the cell assembly. (a) Cell voltage recorded throughout time, (b) polarisation curves measured at the end of break-in, (c) impedance measured at different current densities for the MEA hydrated after cell assembly, (d) impedance measured at different current densities for MEA hydrated before cell assembly, (e) comparison of impedance for both MEAs at 2 A·cm⁻², (f) ohmic resistance and charge transfer resistance calculated after fitting the impedance spectra via an equivalent circuit model. [Correction added on April 2, 2025, after first Online publication: figure 7(f) has been updated in this version.]

further hydrates if it was not fully hydrated before. Therefore, the absence of a change in R_Ω at different current densities of the MEA pre-treated at higher temperature can be attributed to the fact that during the pre-treatment at 90°C, the MEA possibly became fully hydrated.

An increased temperature can not only improve the water absorption of the MEA but also further reduce the contact resistance of materials due to their thermal expansion [23]. However, this effect can only take place if the PTLs have not already reached their maximum compression due to the swelling of the MEA because of their water absorption, and no further reduction in PTL thickness is possible [23]. In this work, the same carbon paper and the same

titanium material were used for the anode and cathode PTLs. But in comparison, the thicknesses of the PTLs, the sealings and the applied clamping pressure are different.

These factors may have an impact on the compression of the PTL layers, and it must be verified for each case individually whether the maximum PTL compression was achieved or not. Based on the measured data, the individual impacts of the protonic conductivity of the membrane and the electrical resistances of the other cell components on the ohmic resistance cannot be accurately resolved. For future experiments, a precise compression measurement of a real operating electrolysis cell should be used to answer this question.

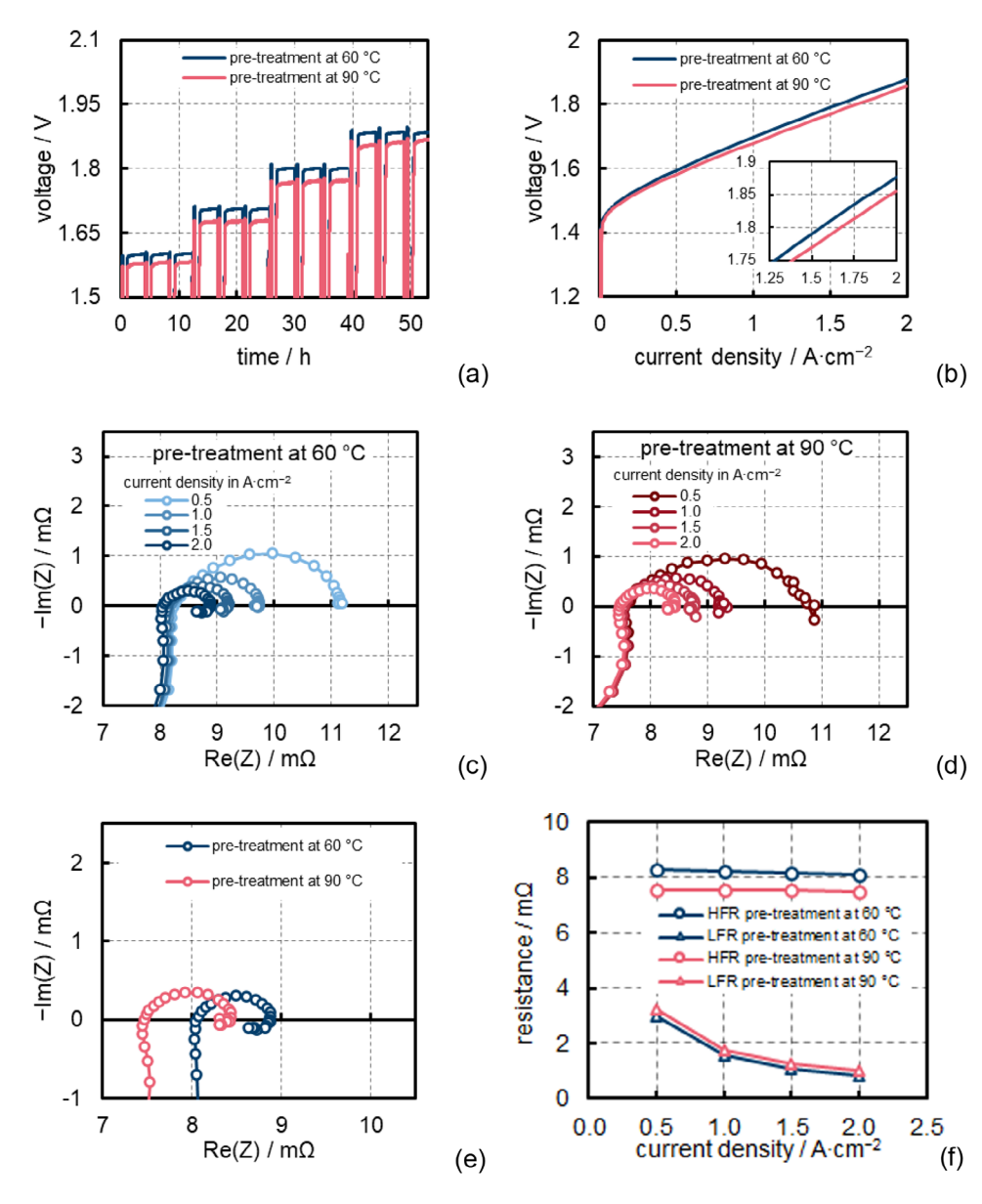


FIGURE 8 Comparison of the break-in procedure between the MEAs pre-treated with deionised water at 60°C (blue) and at 90°C (red) after the cell assembly. (a) Cell voltage recorded throughout time, (b) polarisation curves measured at the end of break-in, (c) impedance measured at different current densities for the MEA hydrated after cell assembly, (d) impedance measured at different current densities for MEA hydrated before cell assembly, (e) comparison of impedance for both MEAs at 2 A·cm⁻² and (f) ohmic resistance and charge transfer resistance calculated after fitting the impedance spectra via an equivalent circuit model. [Correction added on April 2, 2025, after first Online publication: figure 8(f) has been updated in this version.]

3.4 | Overall Comparison

Figure 9 displays the comparison of all pre-treatment procedures applied. The change in cell voltage is drawn from polarisation curves, and ohmic resistance is evaluated from equivalent circuit fittings. In comparison to the MEA pre-treated in situ with water at 60°C, the best performance was obtained by the pre-treatment in situ with acids at 60°C and the pre-treatment in situ with deionised water at 90°C. Only a marginal benefit can be noticed for the pre-treatment at elevated temperatures in comparison to the pre-treatment with acids. However, the acid treatment may influence the characteristics of the other cell components if a high concentration of hydrogen peroxide and sulphuric acid would be used. Comparing only the four pre-treatment procedures investigated in this study, pre-treating the MEA after

cell assembly with deionised water at 90°C seems to be the best way to obtain a high performance of the PEMEC during short-term operation. Nevertheless, these pre-treatment methods are not feasible in large-scale industrial applications according to the current state of the art.

4 | Conclusion

The impact of MEA conditioning on the short-run performance of PEMEC was investigated by comparing mechanical, chemical and thermal conditions during pre-treatment for Nafion N115-based MEAs. Thereby, electrical conditions during the break-in procedure were kept the same for all pre-treatment procedures. The impact of mechanical conditions during pre-treatment was

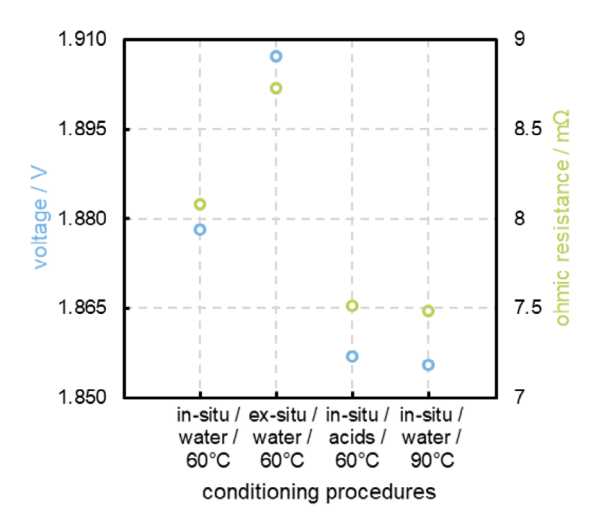


FIGURE 9 | Impact of conditioning procedure on the cell voltage and the ohmic resistance at 2 A-cm^{-2} .

investigated by comparing the application of immersion of the MEA in 60°C deionised water (DI water) before (ex situ) versus after (in situ) assembly of the cell. The impact of chemical treatment was demonstrated by contrasting in situ pre-treatment with DI water versus combined $\rm H_2O_2/H_2SO_4/DI$ -water pre-treatment, both at 60°C. Contrasting juxtaposition considering the impact of thermal pre-treatment conditions covered pre-treatment in DI water at 60°C versus 90°C. The break-in procedure followed a protocol with a gradual increase of the current densities in four equidistant steps from 0.5 to 2.0 A·cm $^{-2}$ for 12 h at each level. Polarisation curves and electrochemical impedance spectra during and right after the break-in procedure were recorded to characterise the electrochemical state of the PEMEC.

In situ pre-treatment, acidic pre-treatment, and elevated 90°C temperature pre-treatment were shown to be favourable for the short-run performance of the PEMEC, as indicated by lower cell voltages in the polarisation curves and lower ohmic resistances, comprising contact resistance and resistance of the membrane. Specifically, when the MEA was pre-treated in situ with DI water after assembling it is in dry state, cell voltage and ohmic resistance were 30 mV and 8.1% lower compared to the ex situ pre-treatment under otherwise the same conditions. This is most likely due to the improvement in contact area and concomitant reduction of the contact resistance resulting from different swelling behaviour of the membrane in a confined environment and underlying the importance of mechanical conditions during pre-treatment. Pretreating the MEA in situ with acidic solution led to a decrease of 21 mV in cell voltage and 7.0% in ohmic resistance compared to the in situ pre-treatment in 60°C DI water, which is most probably due to an increase in the number of mobile protons. Thus, a large part of the improvement in ohmic resistance by the acidic pre-treatment can be ascribed to the reduction in membrane resistance resulting from its enhanced conductivity. Upon pre-treating the MEA in situ with DI water at 90°C rather than 60°C, PEMEC performance was further improved, reaching a 23 mV decrease in cell voltage and 7.4% in ohmic resistance compared to the 60°C pre-treatment. It is possible to correlate this feature to the full hydration of the membrane, confirmed by the constant ohmic resistance at different current densities during the break-in procedure. Thus, most of the improvement along with elevated temperature pre-treatment can be most likely be ascribed to the enhancement in membrane conductivity. According to the EIS evaluation, only minor differences in the charge transfer resistance resulting from the different pre-treatments were detected. It is concluded that at least for the investigated MEA, there is no significant impact of the pre-treatment procedure on the catalyst layer.

The mechanical conditions during pre-treatment affect the contact resistance between MEA and PTL, and chemical conditions and thermal conditions during the pre-treatment, which mainly influence the conductivity of the membrane, have a distinct impact on the performance of a PEMEC. While short-run effects resulting from pre-treatment have been pointed out here, for an optimisation of the conditioning procedure, further investigations of the break-in step and the resulting long-run behaviour remain to be investigated.

Acknowledgements

The authors gratefully acknowledge the financial support by the German Federal Ministry of Education and Research (BMBF) within the $\rm H_2Giga$ project DERIEL (grant number 03HY122C). The authors would also like to thank Zheng Jiang for processing the impedance data.

Conflicts of Interest

The authors declare no conflicts of interest.

Data Availability Statement

The data that support the findings of this study are available from the corresponding author upon reasonable request. The data that supports the findings of this study are available in the supplementary material of this article.

References

- 1. E. Kuhnert, K. Mayer, M. Heidinger, C. Rienessel, V. Hacker, and M. Bodner, "Impact of Intermittent Operation on Photovoltaic-PEM Electrolyzer Systems: A Degradation Study Based on Accelerated Stress Testing," *International Journal of Hydrogen Energy* 55 (2024): 683–695.
- 2. G. Tejera, R. Rojas, E. Teliz, and V. Diaz, "PEM Electrolysis: Degradation Study of N1110 Assemblies for the Production of Green Hydrogen," *Electrochimica Acta* 500 (2024): 144716.
- 3. E. Wallnöfer-Ogris, I. Grimmer, and M. Ranz, "A Review on Understanding and Identifying Degradation Mechanisms in PEM Water Electrolysis Cells: Insights for Stack Application, Development, and Research," *International Journal of Hydrogen Energy* 65 (2024): 381–397.
- 4. M. Sterner and I. Stadler, *Energiespeicher—Bedarf, Technologien, Integration* (Berlin, Heidelberg: Springer, 2017).
- 5. N. Norazahar, F. Khan, N. Rahmani, and A. Ahmad, "Degradation Modelling and Reliability Analysis of PEM Electrolyzer," *International Journal of Hydrogen Energy* 50 (2024): 842–856.
- 6. S. S. Kumar and V. Himabindu, "Hydrogen Production by PEM Water Electrolysis—A Review," *Materials Science for Energy Technologies* 2, no. 3 (2019): 442–454.
- 7. M. S. Kim, J. H. Song, and D. K. Kim, "Development of Optimal Conditioning Method to Improve Economic Efficiency of Polymer Electrolyte Membrane (PEM) Fuel Cells," *Energies* 13, no. 11 (2020): 2831.
- 8. M. Kostelec, M. Gatalo, and N. Hodnik, "Fundamental and Practical Aspects of Break-In/Conditioning of Proton Exchange Membrane Fuel Cells," *Chemical Record* 24, no. 10 (2024): e202400114.

- 9. M. S. Moghaddam, A. Bahari, M. Houshani, A. Jafari, and S. M. T. Tapeh, "A Review on Progress in the Field of Conditioning of Polymer Fuel Cell Stacks," *Journal of Power Sources* 621 (2024): 235300.
- 10. F. van der Linden, E. Pahon, S. Morando, and D. Bouquain, "A Review on the Proton-Exchange Membrane Fuel Cell Break-In Physical Principles, Activation Procedures, and Characterization Methods," *Journal of Power Sources* 575 (2023): 233168.
- 11. S. Pujiastuti and H. Onggo, "Effect of Various Concentration of Sulfuric Acid for Nafion Membrane Activation on the Performance of Fuel Cell." *AIP Conference Proceedings* 1711, no. 1 (2016): 60006.
- 12. K. Christmann, K. A. Friedrich, and N. Zamel, "Activation Mechanisms in the Catalyst Coated Membrane of PEM Fuel Cells," *Progress in Energy and Combustion Science* 85 (2021): 100924.
- 13. M. M. Taghiabadi, M. Zhiani, and V. Silva, "Effect of MEA Activation Method on the Long-Term Performance of PEM Fuel Cell," *Applied Energy* 242 (2019): 602–611.
- 14. W. Wang, K. Li, L. Ding, et al., "Exploring the Impacts of Conditioning on Proton Exchange Membrane Electrolyzers by In Situ Visualization and Electrochemistry Characterization," *ACS Applied Materials & Interfaces* 14, no. 7 (2022): 9002–9012.
- 15. T. Malkow, *EU Harmonised Polarisation Curve Test Method for Low-Temperature Water Electrolysis* (Luxembourg: Publications Office of the European Union, 2018).
- 16. T. Malkow, A. Pilenga, and G. Tsotridis, *EU Harmonised Test Procedure: Electrochemical Impedance Spectroscopy for Water Electrolysis Cells* (Luxembourg: Publications Office of the European Union, 2018).
- 17. G. Tsotridis and A. Pilenga, *EU Harmonised Protocols for Testing of Low Temperature Water Electrolysers* (Luxembourg: Publications Office of the European Union, 2021).
- 18. A. Z. Tomić, I. Pivac, and F. Barbir, "A Review of Testing Procedures for Proton Exchange Membrane Electrolyzer Degradation," *Journal of Power Sources* 557 (2023): 232569.
- 19. S. Siracusano, S. Trocino, N. Briguglio, F. Pantò, and A. S. Aricò, "Analysis of Performance Degradation During Steady-State and Load-Thermal Cycles of Proton Exchange Membrane Water Electrolysis Cells," *Journal of Power Sources* 468 (2020): 228390.
- 20. G. Wei, Y. Wang, C. Huang, Q. Gao, Z. Wang, and L. Xu, "The Stability of MEA in SPE Water Electrolysis for Hydrogen Production," *International Journal of Hydrogen Energy* 35, no. 9 (2010): 3951–3957.
- 21. K. B. Kokoh, E. Mayousse, and T. W. Napporn, "Efficient Multi-Metallic Anode Catalysts in a PEM Water Electrolyzer," *International Journal of Hydrogen Energy* 39, no. 5 (2014): 1924–1931.
- 22. G. Bender, M. Carmo, and T. Smolinka, "Initial Approaches in Benchmarking and Round Robin Testing for Proton Exchange Membrane Water Electrolyzers," *International Journal of Hydrogen Energy* 44, no. 18 (2019): 9174–9187.
- 23. E. Hoppe, S. Holtwerth, M. Müller, and W. Lehnert, "An Ex-Situ Investigation of the Effect of Clamping Pressure on the Membrane Swelling of a Polymer Electrolyte Water Electrolyzer Using X-Ray Tomography," *Journal of Power Sources* 578 (2023): 233242.
- 24. P. Pei, X. Fu, Z. Zhu, P. Ren, and D. Chen, "Activation of Polymer Electrolyte Membrane Fuel Cells: Mechanisms, Procedures, and Evaluation," *International Journal of Hydrogen Energy* 47, no. 59 (2022): 24897–24915.
- 25. E. Padgett, G. Bender, and S. M. Alia, "Membrane Pretreatment and Cell Conditioning for Proton Exchange Membrane Water Electrolysis," *ECS Meeting Abstracts* MA2021-02, no. 41 (2021): 1252.
- 26. S. M. Alia, S. Stariha, and R. L. Borup, "Electrolyzer Durability at Low Catalyst Loading and with Dynamic Operation," *Journal of the Electrochemical Society* 166, no. 15 (2019): F1164–F1172.
- 27. C. Liu, J. A. Wrubel, E. Padgett, and G. Bender, "Impacts of PTL Coating Gaps on Cell Performance for PEM Water Electrolyzer," *Applied Energy* 356 (2024): 122274.

- 28. S. Rodat, S. Sailler, F. Druart, P.-X. Thivel, Y. Bultel, and P. Ozil, "EIS Measurements in the Diagnosis of the Environment within a PEMFC Stack," *Journal of Applied Electrochemistry* 40, no. 5 (2010): 911–920.
- 29. M. R. Gerhardt, L. M. Pant, and J. C. Bui, "Method—Practices and Pitfalls in Voltage Breakdown Analysis of Electrochemical Energy-Conversion Systems," *Journal of the Electrochemical Society* 168, no. 7 (2021): 74503.
- 30. E. Borgardt, L. Giesenberg, and M. Reska, "Impact of Clamping Pressure and Stress Relaxation on the Performance of Different Polymer Electrolyte Membrane Water Electrolysis Cell Designs," *International Journal of Hydrogen Energy* 44, no. 42 (2019): 23556–23567.
- 31. Z. Kang, M. Wang, and Y. Yang, "Performance Improvement Induced by Membrane Treatment in Proton Exchange Membrane Water Electrolysis Cells," *International Journal of Hydrogen Energy* 47, no. 9 (2022): 5807–5816.
- 32. T. A. Zawodzinski, C. Derouin, and S. Radzinski, "Water Uptake by and Transport Through Nafion 117 Membranes," *Journal of the Electrochemical Society* 140, no. 4 (1993): 1041–1047.
- 33. B. Gilois, F. Goujon, A. Fleury, A. Soldera, and A. Ghoufi, "Water Nano-Diffusion Through the Nafion Fuel Cell Membrane," *Journal of Membrane Science* 602 (2020): 117958.
- 34. J. Benziger, A. Bocarsly, M. J. Cheah, P. Majsztrik, B. Satterfield, and Q. Zhao, "Mechanical and Transport Properties of Nafion: Effects of Temperature and Water Activity," in *Fuel cells and hydrogen storage*, ed. A. Bocarsly (Berlin, Heidelberg: Springer, 2011): 85.
- 35. T. D. Gierke, G. E. Munn, and F. C. Wilson, "The Morphology in Nafion Perfluorinated Membrane Products, as Determined by Wide- and Small-Angle X-Ray Studies," *Journal of Polymer Science: Polymer Physics Edition* 19, no. 11 (1981): 1687–1704.
- 36. M. J. Parnian, S. Rowshanzamir, and J. Alipour Moghaddam, "Investigation of Physicochemical and Electrochemical Properties of Recast Nafion Nanocomposite Membranes Using Different Loading of Zirconia Nanoparticles for Proton Exchange Membrane Fuel Cell Applications," *Materials Science for Energy Technologies* 1, no. 2 (2018): 146–154.
- 37. H. Azher, C. A. Scholes, G. W. Stevens, and S. E. Kentish, "Water Permeation and Sorption Properties of Nafion 115 at Elevated Temperatures," *Journal of Membrane Science* 459 (2014): 104–113.
- 38. H. Ito, T. Maeda, A. Nakano, and H. Takenaka, "Properties of Nafion Membranes Under PEM Water Electrolysis Conditions," *International Journal of Hydrogen Energy* 36, no. 17 (2011): 10527–10540.
- 39. T. Schuler, R. de Bruycker, T. J. Schmidt, and F. N. Büchi, "Polymer Electrolyte Water Electrolysis: Correlating Porous Transport Layer Structural Properties and Performance: Part I. Tomographic Analysis of Morphology and Topology," *Journal of the Electrochemical Society* 166, no. 4 (2019): F270–F281.
- 40. T. Schuler, T. J. Schmidt, and F. N. Büchi, "Polymer Electrolyte Water Electrolysis: Correlating Performance and Porous Transport Layer Structure: Part II. Electrochemical Performance Analysis," *Journal of the Electrochemical Society* 166, no. 10 (2019): F555–F565.
- 41. K. Julian, Investigation of the Mechanical Stability of Membranes in Proton Exchange Membrane Water Electrolyzers (Hannover: Institutionelles Repositorium der Leibniz Universität Hannover, 2024).
- 42. T. J. Mason, J. Millichamp, T. P. Neville, A. El-kharouf, B. G. Pollet, and D. J. Brett, "Effect of Clamping Pressure on Ohmic Resistance and Compression of Gas Diffusion Layers for Polymer Electrolyte Fuel Cells," *Journal of Power Sources* 219 (2012): 52–59.
- 43. L. Napoli, M. J. Lavorante, J. Franco, A. Sanguinetti, and H. Fasoli, "Effects on Nafion 117 Membrane Using Different Strong Acids in Various Concentrations," *Journal of New Materials for Electrochemical Systems* 16, no. 3 (2013): 151–156.
- 44. M. Schalenbach, L. Keller, and B. Janotta, "The Effect of Ion Exchange Poisoning on the Ion Transport and Conduction in Polymer Electrolyte

- Membranes (PEMs) for Water Electrolysis," *Journal of the Electrochemical Society* 169, no. 9 (2022): 94510.
- 45. E. Passalacqua, R. Pedicini, and A. Carbone, "Effects of the Chemical Treatment on the Physical-Chemical and Electrochemical Properties of the Commercial Nafion™ NR212 Membrane," *Materials* 13, no. 22 (2020): 5254.
- 46. N. Singhal and A. Datta, "Reversible Tuning of Chemical Structure of Nafion Cast Film by Heat and Acid Treatment," *Journal of Physical Chemistry B* 119, no. 6 (2015): 2395–2403.
- 47. Y. Zhao, K. Yoshimura, T. Motegi, A. Hiroki, A. Radulescu, and Y. Maekawa, "Three-Component Domains in the Fully Hydrated Nafion Membrane Characterized by Partial Scattering Function Analysis," *Macromolecules* 54, no. 9 (2021): 4128–4135.
- 48. J. T. Hinatsu, M. Mizuhata, and H. Takenaka, "Water Uptake of Perfluorosulfonic Acid Membranes from Liquid Water and Water Vapor," *Journal of the Electrochemical Society* 141, no. 6 (1994): 1493–1498.
- 49. A. Parthasarathy, S. Srinivasan, A. J. Appleby, and C. R. Martin, "Temperature Dependence of the Electrode Kinetics of Oxygen Reduction at the Platinum/Nafion Interface—A Microelectrode Investigation," *Journal of the Electrochemical Society* 139, no. 9 (1992): 2530–2537.

Supporting Information

Additional supporting information can be found online in the Supporting Information section.

12 of 12